Active Deformation of Asia: From Kinematics to Dynamics

Philip England* and Peter Molnar

Using estimated strain rates across the actively deforming region of Asia to infer variations in viscous stress, it is shown that gradients of stress point uphill toward the center of Tibet, where gravitational potential energy per unit surface area reaches a maximum. Thus, the dynamics of the deformation seem to obey the equation of creeping flow, which expresses a balance between gradients in stress and the gravitational body force. This balance, in the region of the Tibetan plateau, yields an estimate of 10^{22} pascal second for the average viscosity of the Tibetan lithosphere, which is only about 10 to 100 times greater than the viscosity of the convecting upper mantle.

Plate tectonics gained acceptance 25 to 30 years ago because it passed a simple quantitative test of its central tenet, that the kinematics of surface motions can be described by the rigid-body motions of a small number of plates. A single angular velocity prescribes the relative velocities of all points on any pair of rigid bodies on the surface of a sphere; relative motions measured across the narrow (tens of kilometers wide) bands of intense seismicity and deformation that separate broad regions with little or no seismic activity agreed with the motions expected from the relative rotation of rigid plates, and demonstrated the validity of plate tectonics, at least for the oceanic parts of Earth (*1*).

No comparably simple description of the tectonics of the continents has been accepted. The deformation of continental regions is not confined to narrow bands, but is spread over regions hundreds to thousands of kilometers in horizontal extent. The actively deforming part of Asia, which we consider here, is larger than several of the smaller oceanic plates. The diffuse nature of the deformation led to the inference that the continents, like Earth's mantle, behave as continuously deforming solids, rather than as rigid plates [for example, (*2*–*4*)].

The hypothesis of rigidity of plates was tested by measurements at widely spaced points around the edges of plates (*1*), without the need for measuring velocities in the plate's interior. In contrast, testing the hypothesis that continental deformation is continuous requires knowledge of spatial derivatives of stress, quantities much more difficult to determine than velocities. Furthermore, measurements must be made not only at the boundaries of deforming continents, but throughout entire deforming regions. Making some simplifications to the equation of stress balance in a continuous medium, we carried out a test of its applicability to the tectonics of Asia, estimating the stress field from observations of Quaternary faulting.

Inertial terms are negligible in tectonic processes, so the governing equation for the deformation of a continuous lithosphere is the stress balance equation, which states that gradients of stress are balanced by the force of gravity per unit volume

$$\partial\sigma_{ji}/\partial x_j = -\rho g_i \qquad (1)$$

where σ_{ji} is the ij^{th} component of the stress tensor, x_j is the j^{th} coordinate direction, ρ is the density, and g_i is the i^{th} component of acceleration due to gravity (*5*).

Because neither stress nor strain can be measured at depth within the lithosphere, it is impossible to determine the vertical gradients of stress in Eq. 1 (*6*). We therefore treat deformation of the lithosphere in terms of vertical averages of stress and strain rate in a thin sheet of fluid [for example, (*3*, *4*, *7*)]. This simplification is appropriate where the horizontal dimensions of a region of active deformation exceed by many times the thickness of the lithosphere (*8*).

Gravity anomalies show that, on length scales >100 to 200 km, density contrasts within the lithosphere are isostatically compensated. Thus, the weight per unit area of any column of rock is supported by the vertical traction, σ_{zz}, on its base

$$\sigma_{zz}(z) = -g\int_0^z \rho(z')dz' \qquad (2)$$

where z is depth, z' is a variable of integration, and g is the acceleration due to gravity. With this simplification, σ_{zz} can be specified from a knowledge of the density structure of the lithosphere.

The horizontal equations in Eq. 1 may be expressed in terms of deviatoric stress (*9*), and simplified by taking vertical averages and neglecting shear tractions on the base of the lithosphere [for example, (*10*)]

$$L\,(\partial\tau_{xx}/\partial x - \partial\tau_{zz}/\partial x + \partial\tau_{xy}/\partial y) = \partial\Gamma/\partial x$$
$$\partial\tau_{yy}/\partial y - \partial\tau_{zz}/\partial y + \partial\tau_{xy}/\partial x = \partial\Gamma/\partial y \qquad (3)$$

where L is the thickness of the lithosphere, τ_{ij} is the ij^{th} component of the deviatoric stress tensor, averaged vertically through the lithosphere, and

$$\Gamma = -\int_0^L \sigma_{zz}(z)dz = g\int_0^L\int_0^z \rho(z')dz' \qquad (4)$$

For isostatically balanced columns of lithosphere, differences in Γ are equal to differences in the gravitational potential energy per unit area between columns (*4*, *10*–*12*).

Equation 3 states that horizontal gradients of the deviatoric stress required to deform a thin viscous sheet are balanced by horizontal gradients of its gravitational potential energy (*4*, *7*, *10*, *11*). A simple test of the hypothesis that deformation of the continents is described by this balance would be to determine whether the left-hand side of Eq. 3, derived from observations of deformation, corresponds to gradients of lithospheric potential energy, derived from a knowledge of the density structure of the lithosphere. Because there are no observations of components of vertically averaged stress in the lithosphere and no direct observations of the gravitational potential energy of the lithosphere, we proceeded by using observable proxies for both quantities.

The stresses in Eq. 3 can be related to deformation by specifying a relation between the vertically averaged deviatoric stresses and the vertically averaged strain rates in the lithosphere. The vertical averages of a wide range of possible rheological profiles for the continental lithosphere probably obey a relation of the form

$$\bar{\tau}_{ij} = B\dot{E}^{1/n-1}\dot{\varepsilon}_{ij} \qquad (5)$$

where $\dot{\varepsilon}_{ij}$ is the ij^{th} component of the strain rate, assumed independent of depth

$$\dot{\varepsilon}_{ij} = \frac{1}{2}\left(\frac{\partial u_i}{\partial x_j} + \frac{\partial u_j}{\partial x_i}\right) \qquad (6)$$

where u_i is the i^{th} component of velocity, and $\dot{E} = \sqrt{\dot{\varepsilon}_{ij}\dot{\varepsilon}_{ij}}$, with the convention of summation over repeated subscripts (*13*). Equation 5 expresses the rheology of a "power law" fluid, whose effective viscosity, $1/2B\dot{E}^{1/n-1}$, decreases with increasing magnitude of the strain rate (*13*).

We make the simplifying assumption, which is doubtless wrong in detail, that the variations in components of the average deviatoric stress in the lithosphere, $\bar{\tau}_{ij}$, arise principally from variations in strain rate (that is, we assume B to be constant). With this assumption, we can define a dimensionless stress

P. England, Department of Earth Sciences, Oxford University, Oxford OX1 3PR, UK.
P. Molnar, Department of Earth, Atmospheric, and Planetary Sciences, Massachusetts Institute of Technology, Cambridge, MA 02139, USA.

*To whom correspondence should be addressed. E-mail: philip.england@earth.ox.ac.uk

$$\tau^*_{ij} = \frac{\bar{\tau}_{ij}}{B} \times (1\ \text{sec})^{1/n} = \dot{E}^{1/n-1}\dot{\varepsilon}_{ij} \times (1\ \text{sec})^{1/n} \quad (7)$$

and Eq. 3 becomes

$$\partial\tau^*_{xx}/\partial x - \partial\tau^*_{zz}/\partial x + \partial\tau^*_{xy}/\partial y = \partial\Gamma^*/\partial x$$
$$\partial\tau^*_{yy}/\partial y - \partial\tau^*_{zz}/\partial y + \partial\tau^*_{xy}/\partial x = \partial\Gamma^*/\partial y \quad (8)$$

where

$$\Gamma^* = \Gamma/BL \times (1\ \text{sec})^{1/n} \quad (9)$$

is the dimensionless potential energy of a column of lithosphere.

Γ in Eq. 3 is related to the gravitational potential energy of the whole lithosphere (*11*). Assuming constant crustal density and ignoring lateral variations in the density of the mantle, the difference $\Delta\Gamma$ in gravitational potential energy per unit area between any two isostatically balanced columns of lithosphere is simply

$$\Delta\Gamma = (g\rho_c/2)[1 - (\rho_c/\rho_m)](S_2^2 - S_1^2) \quad (10)$$

where ρ_c and ρ_m are, respectively, the densities of crust and mantle, and S_1 and S_2 are the thicknesses of crust in the two columns. We use Eq. 10 to approximate gravitational potential-energy differences, estimating crustal thickness from surface elevation by assuming isostatic balance with a standard column of oceanic ridge (*14*). We recognize that possible variations in the thickness and temperature structure of the mantle portion of the lithosphere can also contribute to potential-energy contrasts within the lithosphere [see, for example, (*11, 15, 16*)], but these variations are poorly determined in Asia.

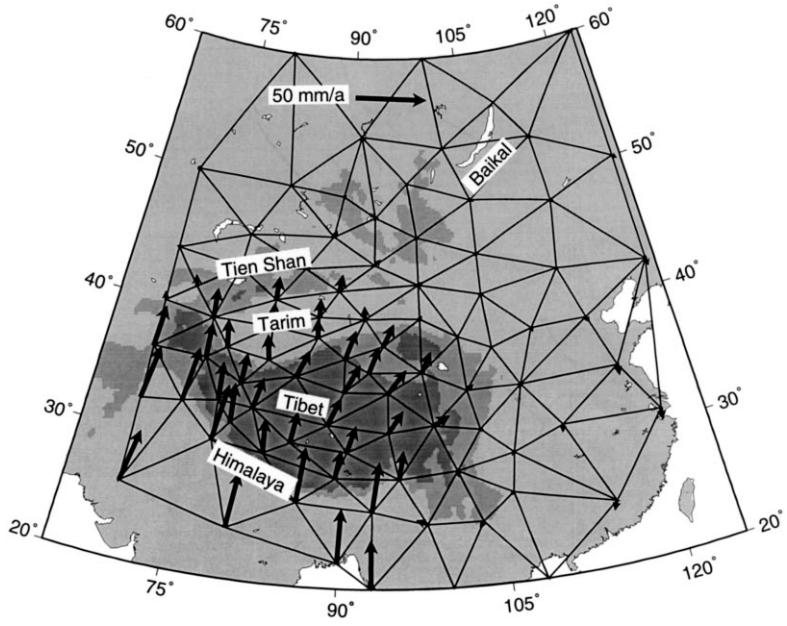

Fig. 1. Field of crustal velocities in Asia [from figure 9 of (*19*)]. Arrows show crustal velocities calculated by integrating estimates of strain rates within triangular regions, derived from Quaternary slip rates on faults. Velocity is shown relative to undeforming Eurasia.

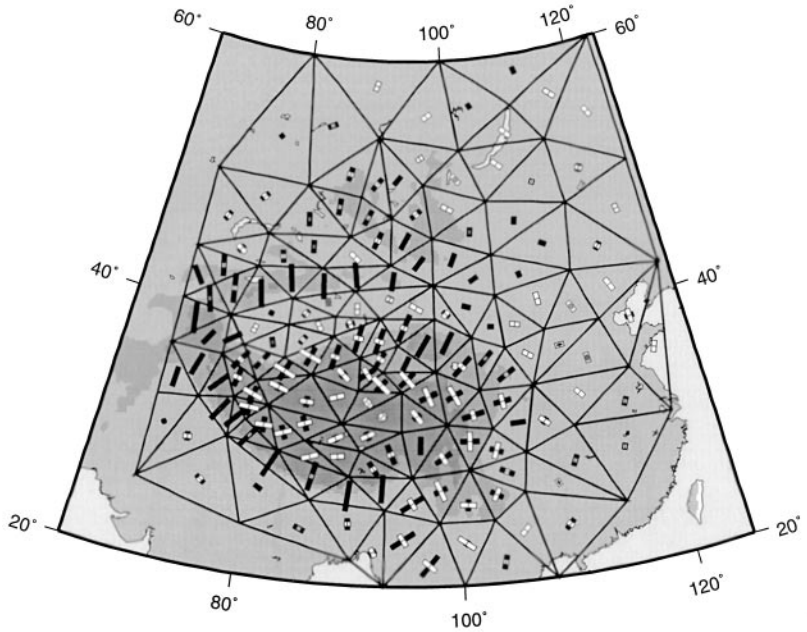

Fig. 2. Strain rates of triangular regions in Asia [from figure 9 of (*19*)], converted to dimensionless stress using Eq. 7, with $n = 3$. Bars show principal horizontal stresses; black bars correspond to contractional stress and white bars to extensional stress. Lengths of symbols are proportional to the magnitude of the respective principal nondimensional stresses (arbitrary scale).

Because logistical and political difficulties preclude the direct measurement of strain rates over the whole of the actively deforming region of Asia, determination of the active strain of this region relies on incomplete information from earthquakes (*17, 18*) and from the rates of slip on faults (*19, 20*). Strain rates estimated from such observations are likely to be inconsistent between neighboring regions, thus forming an unreliable basis for estimating the gradients of strain that are required for the test proposed above.

We circumvented this deficiency [following (*18, 21*)] by imposing on the observations the constraint that the strain rates be self-consistent (or compatible in the sense of St. Venant) in that they should be derivatives of a velocity field (*19, 22*). We covered the region of interest with a mesh of triangles (Fig. 1), in each of which we determined strain rates from estimated Quaternary slip rates of the major faults in Asia, using the method of Kostrov (*23*). We related strain-rate components within each triangle to the relative velocities of its vertices, forming a set of normal equations that could be solved to yield the velocity field (Fig. 1). Self-consistent strain rate components were then derived by differentiation of these velocities.

The most active deformation in eastern Asia occurs within the region 70° to 110°E, and 25° to 55°N, and we restricted our analysis to this region. If the deformation in Asia can be approximated by that of a thin viscous sheet, then the gradients of dimensionless stress in Eq. 8 should point in directions of increasing potential energy, and therefore, approximately uphill on a map of regional topography (Eq. 10).

We converted the self-consistent strain rates into dimensionless stress, using Eq. 7 (see Fig. 2), then interpolated them onto a

regular grid of spacing 2° in latitude and longitude, using a Gaussian smoothing function with a half-width of 200 km. From these gridded data, we constructed the spatial derivatives of dimensionless stresses by standard space-centered finite difference approximations. Estimating the left-hand side of Eq. 8 from these derivatives yields vectors (Fig. 3; arrows) that indeed point uphill around the Tibetan Plateau.

A second comparison can be made by integrating these gradients of dimensionless stresses to yield the dimensionless potential energy (Eqs. 8 and 9). This quantitity reaches its maximum over the Tibetan plateau (Fig. 3), as should be expected if this region deforms, at least approximately, as a viscous sheet (Eq. 3). There is, however, far from perfect agreement between estimated and calculated potential energy in other parts of Asia. For example, large variations of potential energy are calculated in the northeastern part of the region, around Lake Baikal, where the topographic slopes are small, and the calculated potential-energy decreases across the Tien Shan, in disagreement with the increase that is expected from the increase in surface height.

These disagreements may arise because of the simplifing assumptions made in our analysis. To calculate gradients in stress, and estimates of potential energy from these gradients, we assumed that the same rheological parameter B applies to the entire region. Variations in B, as well as influencing the distribution of deformation, would contribute significantly to mismatches in potential energy (*24*); such variations have been suggested among northwest Tibet, the Tarim basin, and the Tien Shan [for example, (*25*)]. The assumption of Airy isostatic compensation to estimate potential energy also introduces an error; variations in potential energy due to lateral variations in the temperature structure of the upper mantle can be as large as those due to changes in crustal thickness (*11, 15*); such variations may affect the region of Mongolia and Lake Baikal, which seems to be underlain by buoyant upper mantle (*26*). The assumption that differences in the potential energy can be determined from differences in surface height works best where crustal thickness variations are largest; in Asia, this is in the region of Tibet. Finally, the application of Eq. 3 implies that basal shear tractions are negligible—a reasonable assumption for Tibet but perhaps not for other regions, such as the Himalaya, where Indian lithosphere is thrust beneath the southernmost Tibetan plateau. For these reasons, we consider the comparisons of potential energy to be meaningful only in the region of Tibet. The potential energy calculated from strain rates and the potential energy calculated from topography are completely independent quantities; agreement between the two in the region of Tibet provides support for the hypothesis that Eq. 3 describes the active deformation there.

If deformation of a homogeneous viscous sheet characterized the tectonics of the region, then estimates of dimensionless potential energy made from the strain-rate field would vary linearly with potential energy estimated from topography, with a slope equal to the value of BL (Eq. 9). Comparison of these two estimates of potential energy per unit area over Asia (Fig. 4) reveals considerable scatter for low areas but a linear trend for the region around Tibet. Assuming $L = 100$ km, the slope of this trend yields an estimate for the spatially averaged rheological parameter, $B = 1.3 \times 10^{12}$ N m^{-2} s$^{1/3}$. For this value of B, the effective viscosity of the lithosphere is approximately 10^{22} N m^{-2} s^{-1} (Table 1). This viscosity, $\sim 10^{22}$ Pa·s, appropriate to a typical strain rate of 10^{-16} to 10^{-15} s^{-1}, is

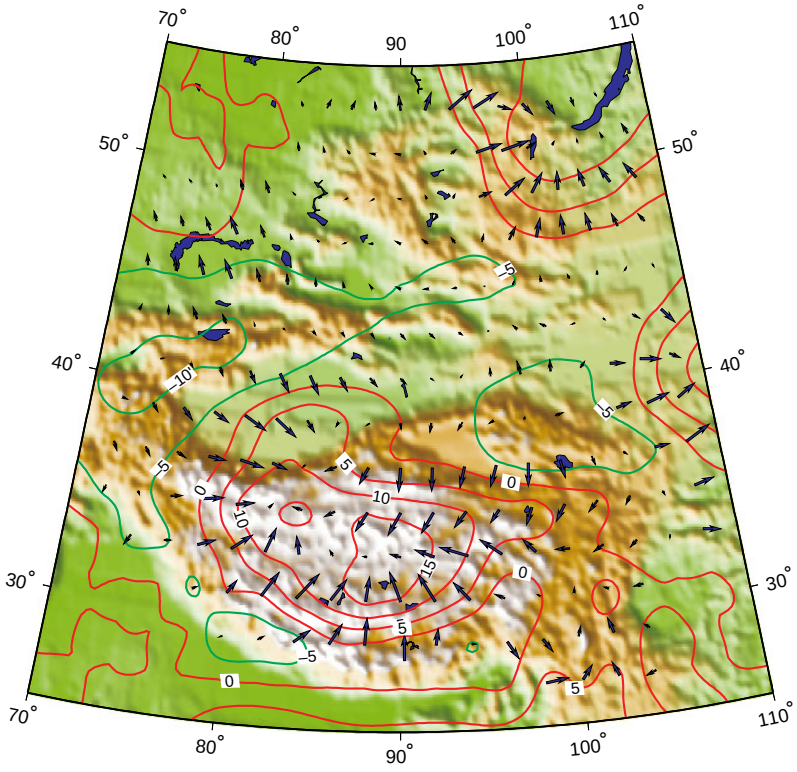

Fig. 3. Arrows show gradients of dimensionless gravitational potential energy, derived by taking the appropriate combinations of derivatives of dimensionless stress, as given by Eq. 8. Lengths of arrows are proportional to the size of the gradients, but scale is arbitrary. Contours show values of dimensionless gravitational potential energy, derived by integrating the gradients of potential energy. Labels on contours show values of dimensionless potential energy (Eq. 9), multiplied by a factor of 10^6.

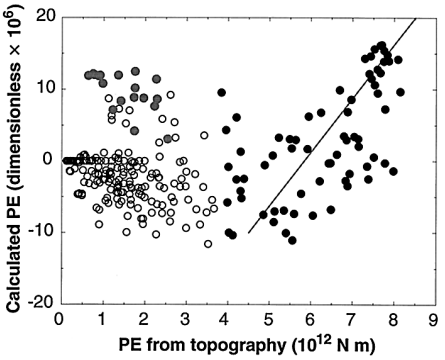

Fig. 4. Calculated dimensionless potential energy (PE) (contours in Fig. 3) against the potential energy calculated from Eq. 10, using observed values of surface height in Asia. Solid symbols are for regions where surface height lies above 3000 m (on the Tibetan plateau), and gray symbols are for the region around Lake Baikal. Open symbols are for the remainder of the region shown in Fig. 3. The straight line has a slope of 1.3×10^{12} N m^{-2} s$^{1/3}$ (*28*).

Table 1. Strain rate ($\dot{\varepsilon} = \dot{E}/\sqrt{2}$), effective viscosity of the lithosphere [$\eta = (1/2)B\dot{E}^{1/n-1}$], and vertically averaged deviatoric stress [$\tau = B\dot{\varepsilon}^{1/n}\sqrt{2}^{(1/n-1)}$], calculated for $B = 1.3 \times 10^{12}$ N m^{-2} s$^{1/3}$ and $n = 3$.

$\dot{\varepsilon}$ (s^{-1})	η (Pa·s)	τ (MPa)
10^{-14}	1.1×10^{21}	22
10^{-15}	5×10^{21}	10
10^{-16}	2×10^{22}	5
10^{-17}	1.1×10^{23}	2

greater than the viscosity of the convecting upper mantle by only one, or at most two, orders of magnitude [for example, (*27*)], suggesting that the continental lithosphere of Asia is more properly regarded as belonging to the fluid portion of the solid earth than to the relatively small fraction of Earth that behaves as rigid plates.

REFERENCES AND NOTES

1. W. Morgan, *J. Geophys. Res.* **73**, 1959 (1968); D. McKenzie and R. Parker, *Nature* **216**, 1276 (1967); C. DeMets, R. G. Gordon, D. F. Argus, S. Stein, *Geophys. J. Int.* **101**, 425 (1990); B. Isacks, J. Oliver, L. Sykes, *J. Geophys. Res.* **73**, 5855 (1968).
2. P. Molnar and P. Tapponnier, *Science* **189**, 419 (1975); P. Tapponnier and P. Molnar, *Nature* **264**, 319 (1976).
3. P. Bird and K. Piper, *Phys. Earth Planet. Inter.* **21**, 158 (1980); P. England and D. McKenzie, *Geophys. J. R. Astron. Soc.* **70**, 295 (1982); P. England, G. Houseman, L. Sonder, *J. Geophys. Res.* **90**, 3551 (1985); J. Vilotte, M. Daignières, R. Madariaga, *ibid.* **87**, 10709 (1982); J. Vilotte, R. Madariaga, M. Daignières, O. Zienkiewicz, *Geophys. J. R. Astron. Soc.* **84**, 279 (1986).
4. P. England and D. McKenzie, *Geophys. J. R. Astron. Soc.* **73**, 523 (1983).
5. We used a left-handed coordinate system, in which *x* is east, *y* is north, and *z* is down. The engineering convention for stresses was used, in which compressional stresses are negative [for example, L. Malvern, *Introduction to the Mechanics of a Continuous Medium* (Prentice-Hall, Englewood Cliffs, NJ, 1969)].
6. We recognize the abundant evidence for rheological layering in the lithosphere and the theoretical arguments [for example, P. Bird, *J. Geophys. Res.* **96**, 10275 (1991); L. H. Royden *et al.*, *Science* **276**, 788 (1997)] that such layering may play an important role in deformation of Tibet. Because, however, the measurement of subsurface kinematics, let alone dynamics, is impossible, we confined our analysis to a simple structure.
7. G. Houseman and P. England, *J. Geophys. Res.* **91**, 3651 (1986).
8. The development follows that of (*4*) and (*10*), to which readers are referred for details.
9. The deviatoric stress tensor, τ, is defined by $\tau_{ij} = \sigma_{ij} - (1/3)\sigma_{kk}$ with the convention of summation over repeated subscripts. $(1/3)\sigma_{kk}$ (the negative of the pressure) is generally unimportant in the rheology of rocks of the lithosphere.
10. P. England and J. Jackson, *Annu. Rev. Earth Planet. Sci.* **17**, 197 (1989).
11. P. Molnar and H. Lyon-Caen, *Geol. Soc. Am. Spec. Pap.* **218**, 179 (1988); P. Molnar, P. England, J. Martinod, *Rev. Geophys.* **31**, 357 (1993).
12. We neglected basal tractions, though they may be incorporated in an analysis if an adequate method is available for specifying such tractions from observations [S. Wdowinski, R. O'Connell, P. England, *J. Geophys. Res.* **94**, 10331 (1989); S. Ellis, P. Fullsack, C. Beaumont, *Geophys. J. Int.* **120**, 24 (1995)].
13. L. Sonder and P. England [*Earth Planet. Sci. Lett.* **77**, 81 (1986)] show that Eq. 5 represents the vertical average, throughout the lithosphere, of several mechanisms, including frictional slip on faults in the upper 10 to 20 km of the crust and power-law creep with $n \sim 3$ in the deeper levels of the lithosphere, where ductile deformation occurs [J. Weertman, *Rev. Geophys. Space Phys.* **8**, 145 (1970)]. No unambiguous physical significance can be assigned to *n* in Eq. 5, but as a rule of thumb, *n* lies close to 3 where the strength of the lithosphere is dominated by its ductile layer and increases as the contribution to strength made by faults in the upper crust increases (*13*).
14. We calculated potential energies following the procedure of [(*15*), appendix], assuming that crust 35 km thick has a surface height of 250 m and that the lithosphere thickness is 100 km. The influence of varying these values, respectively, between 30 and 45 km, and between 100 and 200 km, is to change the quantities derived in this paper (Figs. 3 and 4; Table 1) by less than 50%.
15. P. England and G. Houseman, *J. Geophys. Res.* **94**, 17561 (1989).
16. C. Jones, J. Unruh, L. Sonder, *Nature* **381**, 37 (1996).
17. P. Molnar and Q. Deng, *J. Geophys. Res.* **89**, 6203 (1984); J. Jackson and D. McKenzie, *Geophys. J. Int.* **93**, 45 (1988); G. Ekström and P. England, *J. Geophys. Res.* **94**, 10231 (1989).
18. W. E. Holt, J. F. Ni, T. C. Wallace, A. J. Haines, *J. Geophys. Res.* **96**, 14595 (1991); W. E. Holt, M. Li, A. J. Haines, *Geophys. J. Int.* **122**, 569 (1995).
19. P. England and P. Molnar, *Geophys. J. Int.* **130**, 557 (1997).
20. G. Peltzer and F. Saucier, *J. Geophys. Res.* **101**, 27943 (1996).
21. A. J. Haines, *Geophys. J. R. Astron. Soc.* **68**, 203 (1982); _____ and W. E. Holt, *J. Geophys. Res.* **98**, 12057 (1993); J. Jackson, A. J. Haines, W. Holt, *ibid.* **97**, 17657 (1992); _____, *ibid.* **100**, 15205 (1995).
22. St. Venant's equations of strain compatibility derive from the definitions of strain rates as derivatives of the components of velocity, for example, Eq. 6. Thus, strain rates derived by differentiating the components of a velocity field are internally consistent throughout the region where the velocity field is known, whereas strain rates estimated piecemeal from faulting or earthquakes need not be consistent with each other [for example, (*21*)].
23. B. Kostrov, *Izv. Acad. Sci. USSR Phys. Solid Earth* **97**, 23 (1974).
24. To appreciate the influence of variations of *B* on estimates of potential energy, consider a one-dimensional rendition of Eq. 3: $L\partial\bar{\tau}_{xx}/\partial x = \partial\Gamma/\partial x$. With variation in *B* and approximation of derivatives by differences over a unit length, we can write: $LB\Delta\dot{\varepsilon}_{xx}^{1/n} + L\dot{\varepsilon}_{xx}^{1/n}\Delta B \approx \Delta\Gamma$. For $L = 100$ km, $\dot{\varepsilon}_{xx} = 10^{-15}$ s^{-1}, and $n = 3$, the potential energy associated with the neglected second term on the left-hand side of this equation is $\Delta\Gamma \approx \Delta B$. Therefore, neglecting ΔB of order *B* is equivalent to introducing a spurious potential energy of order *B* ($\approx 2 \times 10^{12}$ N m^{-1}; Fig. 4).
25. P. Molnar and P. Tapponnier, *Earth Planet. Sci. Lett.* **52**, 107 (1981); J. Vilotte, M. Daignières, R. Madariaga, O. Zienkiewicz, *Phys. Earth Planet. Inter.* **36**, 236 (1984); P. England and G. Houseman, *Nature* **315**, 297 (1985); E. A. Neil and G. A. Houseman, *Tectonics* **16**, 571 (1997).
26. N. A. Logatchev, Y. A. Zorin, V. A. Rogozhina, *Tectonophysics* **94**, 223 (1983); I. Baljinnyam *et al.*, *Geol. Soc. Am. Mem.* **181**, (1993).
27. J. Mitrovica, *J. Geophys. Res.* **101**, 555 (1996); _____ and A. Forte, *ibid.* **102**, 2751 (1997).

28. Funded in part by the National Environment Research Council (U.K.) grant GR3/9183 to P.E., who is grateful for support from the Division of Geological and Planetary Sciences, California Institute of Technology, while part of this work was carried out. Also supported by NSF under grant EAR9527024 to P.M. Figures were produced with GMT [P. Wessel and W. H. F. Smith, *Eos* **76**, 329 (1995)], and the text was prepared with GNUemacs.

29 May 1997; accepted 12 September 1997

Deformation in the Lower Crust of the San Andreas Fault System in Northern California

Timothy J. Henstock, Alan Levander, John A. Hole

A continuous seismic velocity and reflectivity cross-section of the San Andreas fault system in northern California shows offsets in the lower crust and the Mohorovičić Discontinuity near the San Andreas and Maacama strike-slip faults. These faults may cut through the crust to the upper mantle in a zone less than 10 kilometers wide. The northern California continental margin to the eastern edge of the Coast Ranges is underlain by a high-velocity lowermost crustal layer that may have been emplaced within 2 million years following the removal of the Gorda plate slab. The rapid emplacement and structure within this layer are difficult to reconcile with existing tectonic models.

The relation between deformation in the crust and mantle is uncertain. A key area in which to examine this relation is the San Andreas fault fault system (SAFS) in northern California. Here, the SAFS includes the San Andreas fault (SAF), Maacama fault (MF), and Bartlett Springs fault (BSF). We wish to know whether the faults cut directly through the crust and into the mantle, or whether the upper crustal faults are linked by sub-horizontal detachments to the lower crust and mantle, so that motion in the mantle is not directly coupled to that in the overlying crust. The development of the SAFS is related to the migration of the Mendocino Triple Junction (MTJ) (*1*). As the MTJ migrated northward, the Gorda slab is thought to have been removed from beneath northern California and replaced by the upwelling of asthenospheric mantle (*2*).

Here, we present results from the 1993 and 1994 MTJ seismic experiments (*3*, *4*) along an east-west line at latitude 39.4°N extending from the Pacific Ocean basin to the eastern side of the Coast Ranges (Fig. 1A). Gravity (*5*), teleseismic (*6*), and crustal seismic data (*4*) suggest that the southern edge of the Gorda slab lies 50 to 100 km to the north of the profile. Recent volcanism, dated at 2 Ma, in the Clear Lake region 50 to 100 km to the south of the profile has been attributed to upwelling in the wake of MTJ migration (*7*).

We developed a *P*-wave seismic velocity model using the travel times (*8*) of reflected and refracted arrivals from land, marine, and onshore-offshore recordings (Fig. 1C). The seismic velocity model shows that the upper-

T. J. Henstock and A. Levander, Department of Geology and Geophysics, MS-126, Rice University, Houston, TX 77005–1892, USA.
J. A. Hole, Department of Geological Sciences, Virginia Polytechnic Institute, Blacksburg, VA 24061–0420, USA.